

# Simulation of pulsed CO<sub>2</sub> laser second harmonic generation in nonlinear ternary semiconductor crystals with the allowance for thermal blooming

P.P. Geiko

*Institute of Optical Monitoring,  
Siberian Branch of the Russian Academy of Sciences, Tomsk*

Received May 5, 2003

Possibilities of developing high-efficiency and high-output second harmonic generators for mini TEA CO<sub>2</sub> laser are studied. The system of shortened equations for interacting waves along with the two-dimensional heat conduction equation is solved. These equations describe second harmonic generation (SHG) taking into account the effect of thermal blooming. The efficiency of SHG with ZnGeP<sub>2</sub>, CdGeAs<sub>2</sub>, AgGaSe<sub>2</sub>, HgGaS<sub>4</sub>, Tl<sub>3</sub>AsSe<sub>3</sub>, and GaSe nonlinear crystals was estimated depending on the crystal length and optical quality. The following CO<sub>2</sub> pump laser parameters were used: wavelength of 9.55 μm, pulse energy of 50 mJ, pulse duration from 1 to 100 ns, pulse repetition rate up to 1 kHz. The additional angular tuning of the crystals that maximizes SHG efficiency as well as the optimal crystal lengths providing for its maximum at a fixed pump pulse repetition rate were determined as well. The possibility of developing second harmonic generators with high (up to tens of watts) mean power has been proposed.

## Introduction

Thanks to high performance characteristics and the possibilities of operating as a part of mobile and onboard systems, repetitively pulsed TEA CO<sub>2</sub> lasers are widely used in lidars designed for laser monitoring of the atmosphere. Development of high-efficiency crystal frequency converters allows one not only to improve the parameters of existing lidar systems, but also to extend significantly the scope of solved problems. Prominent examples are second harmonic generators (SHG) of the 9-μm band that extend the list of gases monitored by CO<sub>2</sub>-laser based gas analyzers.<sup>1-3</sup>

The aim of this work was to assess the feasibilities of achieving high-efficiency SHG of the radiation of repetitively pulsed TEA CO<sub>2</sub> lasers suitable for operation as a part of mobile lidars.

However, the choice of the best crystal even for this particular problem is not obvious. Important parameters determining, for example, the degree of development of the disturbing thermal processes (heat conductivity) and drift of interacting radiations (birefringence), are determined quite correctly by now. However, these are quite different for different crystals and therefore cause uncertainty. This follows from the Table of basic properties determining the frequency doubling efficiency for six nonlinear crystals that are now most promising for solution of the problem formulated above. Some of these data on the general physical properties of the crystals were borrowed from Ref. 4, and the measured values of the surface damage threshold were taken from Ref. 5. Note that the damage threshold was determined for

30-ns long pulses. The data given in the Table were used in the subsequent calculations.

The SHG efficiency reaches its maximum when the phase matching conditions are fulfilled for the interacting waves. The fulfillment can be obtained by selecting pump wave polarization and the angle between the direction of pump wave propagation and the optical axis of the crystal. The nonlinear figure of merit  $M = d_{\text{eff}}^2 / (n_1^2 n_2)$  is one of the key parameters determining the frequency conversion efficiency. Here  $d_{\text{eff}}$  is the effective nonlinear susceptibility, which is determined with the allowance for the phase-matching angles and the type of symmetry of a crystal;  $n_1$  and  $n_2$  are the refractive indices at the pump and second harmonic frequencies.

Figure 1 depicts the spectral dependences of the phase-matching angles and the nonlinear figures of merit for the crystals under study calculated using the Sellmeier equations.<sup>4</sup> Regardless of an obvious advantage of CdGeAs<sub>2</sub> crystal over the other crystals in the figure of merit, it should be noted that this crystal has the highest absorption at the pump and second harmonic wavelengths due to free carriers. To decrease this absorption down to the level of 0.3–0.5 cm<sup>-1</sup>, cryogenic cooling down to 77 K is usually used, and this significantly deteriorates the operating ability and restricts possible length of the crystals. It can be seen from Fig. 1b that at doubling of the 9-μm band of a CO<sub>2</sub> laser the ZnGeP<sub>2</sub> crystal must exceed AgGaSe<sub>2</sub> in efficiency, simultaneously being inferior to it at SHG of the 10-μm branch. In the ZnGeP<sub>2</sub> crystal it is also possible to change the phase matching conditions and to control them by heating the crystal (this is described in detail in Ref. 6).

Parameters of nonlinear crystals – doublers of CO<sub>2</sub> laser frequency

Parameter	Crystal					
	ZnGeP <sub>2</sub>	CdGeAs <sub>2</sub>	AgGaSe <sub>2</sub>	HgGa <sub>2</sub> S <sub>4</sub>	Tl <sub>3</sub> AsSe <sub>3</sub>	GaSe
Symmetry group	$\bar{4}2m(+)$	$\bar{4}2m(+)$	$\bar{4}2m(-)$	$\bar{4}(-)$	$3mm(-)$	$6m2(-)$
Type of phase matching	eeo	eeo	ooe	ooe	ooe	ooe
Phase-matching angles, degs	63–90	32.9–33.8	71.1–56.5	65–90	18.5–19.3	10.7–12.4
$n_{1o}, n_{1e},$	3.07 3.10	3.51 3.60	2.60 2.57	2.38 2.34	3.34 3.16	2.82 2.45
$n_{2o}, n_{2e}$	3.10 3.14	3.54 3.63	2.62 2.59	2.42 2.37	3.36 3.17	2.84 2.46
Nonlinear coefficient $d$ , pm/V	$d_{14} = 75$	$d_{14} = 236$	$d_{36} = 39$	$d_{36} = 35.2$ $d_{31} = 11.7$	$d_{15} = 66$ $d_{22} = 32$	$d_{22} = 54$
Effective nonlinear susceptibility, $d_{\text{eff}}$ , pm/V	$[d_{14}\sin(2\theta) \times \cos(2\phi)]$	$[d_{14}\sin(2\theta) \times \cos(2\phi)]$	$[d_{36}\sin(\theta) \times \sin(2\phi)]$	$[d_{36}\sin(\theta) \times \sin(2\phi) + d_{31}\sin(\theta) \times \cos(2\phi)]$	$[d_{15}\sin(\theta) - d_{22}\cos(\theta) \times \sin(3\phi)]$	$[d_{22}\cos(\theta) \times \sin(3\phi)]$
$dn_e/dT$ , K <sup>-1</sup> · 10 <sup>5</sup>	16.1	21.5	8.36	–	3.55	–
$dn_o/dT$ , K <sup>-1</sup> · 10 <sup>5</sup>	14.7	24.3	8.1	–	–4.52	15
Heat conductivity $\kappa$ , W/(cm · K) · 10 <sup>3</sup>	0.36	0.067	0.01	–	0.0035	0.162
Heat capacity $C$ , J/(g · K)	0.463	0.3	0.3	–	0.19	0.35
Density $\rho$ , g/cm <sup>3</sup>	4.158	5.72	5.71	4.95	7.83	5.03
Linear absorption coefficient, cm <sup>-1</sup>						
$2\delta_1$	0.36	0.1	0.01	0.2	0.005	0.05
$2\delta_2$	0.01	0.5	0.005	0.1	0.005	0.05
Damage threshold $I_d$ , MW/cm <sup>2</sup>	142	157	139	294	132	121

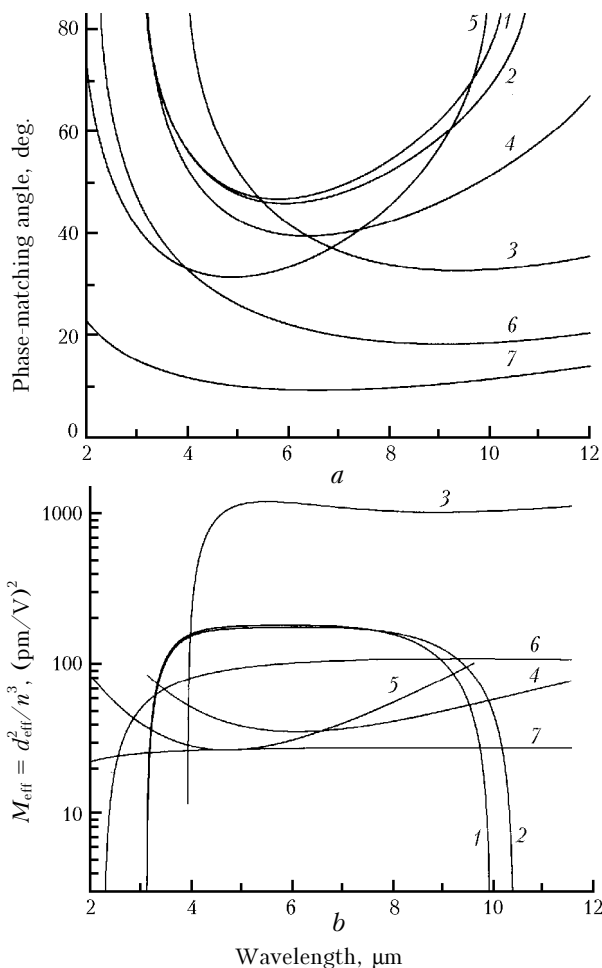


**Fig. 1.** Spectral dependences of the phase-matching angles and figures of merit for SGH using type I of the interaction at  $T = 300$  K in nonlinear crystals: ZnGeP<sub>2</sub> (1), ZnGeP<sub>2</sub> [ $T = 500$  K] (2), CdGeAs<sub>2</sub> (3), AgGaSe<sub>2</sub> (4), HgGa<sub>2</sub>S<sub>4</sub> (5), Tl<sub>3</sub>AsSe<sub>3</sub> (6), and GaSe (7).

## 1. Mathematical model of pulsed SHG

Using standard paraxial approximation of the wave equation, one can obtain the following system of equations for the complex amplitudes of the pump wave  $A_1$  and second harmonic  $A_2$  (Ref. 7):

$$\frac{\partial A_1}{\partial z} - \frac{1}{2ik_1} \left( \frac{\partial^2 A_1}{\partial x^2} + \frac{\partial^2 A_1}{\partial y^2} \right) + \beta_1 \frac{\partial A_1}{\partial x} + \delta_1 A_1 = -i\sigma_1 A_1^* A_2 \exp(-i\Delta k z), \quad (1)$$

$$\frac{\partial A_2}{\partial z} - \frac{1}{2ik_2} \left( \frac{\partial^2 A_2}{\partial x^2} + \frac{\partial^2 A_2}{\partial y^2} \right) + \beta_2 \frac{\partial A_2}{\partial x} + \delta_2 A_2 = -i\sigma_2 A_1^2 \exp(i\Delta k z).$$

Here  $k_1$  and  $k_2$  are wave numbers of the pump and SH waves;  $\Delta k = k_2 - 2k_1$  is the wave mismatch;  $\beta_{1,2}$ ,  $\delta_{1,2}$ ,  $\sigma_{1,2} = 4\pi k_1 d_{1,2\text{eff}} / n^2(\omega_{1,2})$  are the walk off angles, linear absorption coefficients, and the coefficients of nonlinear coupling, respectively. In this case, if the frequencies  $\omega_1$  and  $\omega_2$  are far from characteristic fundamental absorption bands (just this is the case most interesting in practice), the additional Kleinman symmetry conditions are valid and the values of  $d_{1\text{eff}}$  and  $d_{2\text{eff}}$  coincide.<sup>8</sup> Any physical effect can be taken into account in Eqs. (1) by introducing the appropriate term.<sup>9</sup> In addition to linear absorption, Eqs. (1) take into account the walk off of the energy of interacting beams (diaphragm aperture effect) caused by birefringence. It decreases the efficiency of SH conversion, especially, at small cross sections of the pump beam and in long crystals. This effect is described in Eq. (1) by the terms with the first derivative with respect to the cross coordinate  $x$  and the walk off angles  $\beta$  determined by the equation

$$\beta \approx \tan\theta = \sin(2\theta) [(n_o - n_e)/n_o], \quad (2)$$

where  $\theta$  is the phase-matching angle;  $n_o$  and  $n_e$  are the refractive indices for the ordinary and extraordinary waves. The factor  $\exp(\pm i\Delta kz)$  describes the effect of phase mismatch of the interacting waves on the conversion efficiency.

In the process of parametric frequency conversion, some energy of the interacting radiations is absorbed thus causing heating of the crystal. This is taken into account in Eqs. (1) by the terms proportional to the linear absorption coefficients. Because of the inhomogeneous intensity distribution in the pump beam, inhomogeneous heating occurs across a crystal. This heating is characterized by the temperature distribution  $T(x, y) = \Delta T(x, y) + T_s$ , where  $T_s$  is the temperature of the lateral surface of the crystal,  $\Delta T(x, y)$  is the spatially inhomogeneous addition. At transition through the lateral surface of the crystal, the temperature jump  $T_s - T_0$  is observed ( $T_0$  is the thermostat temperature) along with the associated heat flux from the crystal to the thermostat. In the further consideration, we will take into account only spatially inhomogeneous component  $\Delta T(x, y)$  of  $T(x, y)$ , since thermal refraction arises due to the cross temperature gradients, and the homogeneous part of the thermal mismatch of phase matching can be compensated for by turning the crystal.<sup>7</sup> In Refs. 10 and 11, the three-dimensional heat conduction equation was solved in a system of cylindrical coordinates and it was shown that the longitudinal temperature gradients can be neglected.

Inhomogeneous heating of the crystal leads to spatially inhomogeneous distribution of the refractive indices of the interacting radiations. As this takes place, the inhomogeneous (over the beam cross section) phase mismatch and the spatially inhomogeneous dispersion birefringence  $B = n_e(\theta) - n_o$  arise, and this limits the efficiency of the process. Unlike the single pulse mode, in the repetitively pulsed mode the thermal effects are accumulated and have the decisive effect on the frequency conversion process.

Having in mind the above-said, the account of thermal blooming effect of laser beams assumes supplementing the system of equations (1) with the two-dimensional heat conduction equation and introducing the expressions ( $i\gamma_{1,2}TA_{1,2}$ ) determining these effects. The resulting system of equations for calculation of the SHG efficiency takes the form:

$$\begin{aligned} \frac{\partial A_1}{\partial z} - \frac{1}{2ik_1} \left( \frac{\partial^2 A_1}{\partial x^2} + \frac{\partial^2 A_1}{\partial y^2} \right) + \beta_1 \frac{\partial A_1}{\partial x} + \delta_1 A_1 + i\gamma_1 T A_1 &= \\ &= -i\sigma_1 A_1^* A_2 \exp(-i\Delta kz), \\ \frac{\partial A_2}{\partial z} - \frac{1}{2ik_2} \left( \frac{\partial^2 A_2}{\partial x^2} + \frac{\partial^2 A_2}{\partial y^2} \right) + \beta_2 \frac{\partial A_2}{\partial x} + \delta_2 A_2 + i\gamma_2 T A_2 &= \\ &= -i\sigma_2 A_{1,2}^2 \exp(i\Delta kz), \end{aligned} \quad (3)$$

$$\frac{\partial T}{\partial t} = \chi \left( \frac{\partial^2 T}{\partial x^2} + \frac{\partial^2 T}{\partial y^2} \right) + \frac{cn}{4\pi\rho C_p} (\delta_1 |A_1|^2 + \delta_2 |A_2|^2),$$

where  $\gamma_{1,2} = k_{1,2} \frac{\partial n_{1,2}}{\partial T}$  is the coefficient responsible for thermal blooming;  $\chi = \kappa/(\rho C_p)$  is the thermal diffusivity;  $T$  is the excess of the crystal temperature over the ambient temperature;  $\kappa$  is the heat conductivity;  $\rho$  is the density;  $C_p$  is the specific heat.

The system of equations (3) is complemented by the boundary and initial conditions. The distribution of the pump wave entering the crystal is set in accord with the intensity distribution over the cross section of the pump beam. In calculations we used model rectangular pulses and pulses with the Gaussian distribution

$$\begin{aligned} A(x, y, t) &= A_1(x, y, z = 0, t) = A^0(x, y, t) = \\ &= A^0 \left( \frac{2}{\pi^{3/2} \tau w^2} \right)^{1/2} \exp(-(x^2 + y^2)/2w^2) \exp(-2t^2/\tau^2). \end{aligned} \quad (4)$$

Here  $w$  is the effective beam radius at the  $1/e$  level;  $\tau$  is the duration of the pump pulse at the  $1/e$  power level;  $A^0$  is the amplitude of the pump. For the second harmonic wave it was taken that  $A_2(x, y, z = 0, t) = 0$ , as is the general case for the fields beyond the crystal, that is,

$$\begin{aligned} A_{1,2}(0, y, z, t) &= 0, \quad A_{1,2}(x, 0, z, t) = 0, \\ A_{1,2}(L_x, y, z, t) &= 0, \quad A_{1,2}(x, L_y, z, t) = 0, \end{aligned} \quad (5)$$

where  $L_x \times L_y \times L_z$  are the dimensions of the nonlinear crystal. The initial temperature of the crystal was taken equal to the ambient one, that is,  $T(x, y, z, t = 0) = 0$ . Heat exchange with the coefficient  $\alpha$  was assumed to proceed through the lateral surface, that is,

$$\begin{aligned} \kappa(\partial T / \partial x) + \alpha T|_{x=L_x} &= 0, \quad -\kappa(\partial T / \partial x) + \alpha T|_{x=0} = 0, \\ \kappa(\partial T / \partial y) + \alpha T|_{y=L_y} &= 0, \quad -\kappa(\partial T / \partial y) + \alpha T|_{y=0} = 0. \end{aligned}$$

The system of equations (3) with the above boundary and initial conditions describes the following physical effects influencing the SHG efficiency:

- 1) pump depletion (energy transfer from the pump wave to the second harmonic wave);
- 2) absorption of the pump and second harmonic waves;
- 3) energy walk off of the pump beam or the second harmonic wave;
- 4) diffraction blooming of the beam;
- 5) inhomogeneous heating along the cross coordinates;
- 6) thermal blooming of the pump beam and SH beam.

## 2. Technique for calculation of SHG efficiency

Having passed to dimensionless variables and introduced the following designations:

$$\begin{aligned}\zeta &= z/L_z, \quad \xi = x/L_x, \quad v = y/L_y, \quad d = L_z/(2k_1L_{x,y}), \\ u_{1,2} &= A_{1,2}/A^0, \quad \Delta = \Delta kL_z, \quad \tilde{\beta}_{1,2} = \beta_{1,2}L_z/L_x, \quad g = L_z/l_{nl}, \\ \tilde{\delta}_{1,2} &= \delta_{1,2}L_z, \quad \tilde{\tau}_T = L_{x,y}/\chi, \quad T^0 = 2\delta_1 I_t(0) \quad \tilde{\tau}_T / (\rho C_p), \\ \tilde{\gamma}_{1,2} &= \gamma_{1,2}L_z T^0, \quad \tau = t/\tilde{\tau}_T, \quad \tilde{T} = T/T^0, \quad (6)\end{aligned}$$

we obtain the system of equations:

$$\begin{aligned}\frac{\partial u_1}{\partial \zeta} + id \left( \frac{\partial^2 u_1}{\partial \xi^2} + \frac{\partial^2 u_1}{\partial v^2} \right) + \tilde{\beta}_1 \frac{\partial u_1}{\partial \xi} + \tilde{\delta}_1 u_1 + i\tilde{\gamma}_1 \tilde{T} u_1 &= \\ &= -igu_1^* u_2 \exp(-i\Delta\zeta), \\ \frac{\partial u_2}{\partial \zeta} + \frac{id}{2} \left( \frac{\partial^2 u_2}{\partial \xi^2} + \frac{\partial^2 u_2}{\partial v^2} \right) + \tilde{\beta}_2 \frac{\partial u_2}{\partial \xi} + \tilde{\delta}_2 u_2 + i\tilde{\gamma}_2 \tilde{T} u_2 &= \\ &= -igu_1^2 \exp(i\Delta\zeta), \quad (7) \\ \frac{\partial \tilde{T}}{\partial \tau} &= \frac{\partial^2 \tilde{T}}{\partial \xi^2} + \frac{\partial^2 \tilde{T}}{\partial v^2} + |u_1|^2 + (\tilde{\delta}_2 / \tilde{\delta}_1) |u_2|^2.\end{aligned}$$

The basic idea of the numerical method used for solution of this system of equations consists in approximating the continuous nonlinear medium by a set of equidistant layers, each characterized by an equivalent complex enhancement factor. The medium between layers has no enhancement factor. The field propagation between the layers is described using the Fourier transform. For this purpose, it is reasonable to use Fast Fourier Transform (FFT) algorithms, which are less time-consuming as compared to alternative finite-difference methods for solution of nonlinear parabolic equation.<sup>12,13</sup>

The first two equations can be written as

$$\frac{\partial u_j}{\partial \zeta} + id_j \left( \frac{\partial^2 u_j}{\partial \xi^2} + \frac{\partial^2 u_j}{\partial v^2} \right) + \tilde{\beta}_j \frac{\partial u_j}{\partial \xi} = f_j. \quad (8)$$

Here  $d_1 = d$ ,  $d_2 = d/2$ .

The numerical solution of Eqs. (8) was reduced to successive integration of homogeneous equations (propagation of the fields  $u_{1,2}$  through the free space at a distance  $\Delta\zeta$ ) using FFT with the allowance made for the walk off and integration of the equations

$$du_j/d\zeta = f_j. \quad (9)$$

at each  $\zeta_s$  layer by the Runge-Kutta method.

To decrease the number of terms and increase the computation speed, the terms describing blooming were not included in  $f_j$ , but taken into account by introducing phase screens  $\exp(-i\gamma\tilde{T}\Delta\zeta)$  at each  $\zeta_s$  layer.

Numerical simulation of the SHG has been carried out in two modes: single pulse mode and repetitively pulsed mode with the allowance for the processes of temperature field establishment in a crystal. When simulating numerically the propagation of the fields  $u_{1,2}(\xi, v)$  by the FFT method, it is necessary to specify the interval  $G = L_{x,y}/2w$  to meet the boundary conditions and the number of grid points ( $N_\xi, N_v$ ) for representation of the functions of cross coordinates  $\xi$  and  $v$ . The appropriate values of  $G$  and ( $N_\xi, N_v$ ) are determined by the Fresnel number of the problem under consideration and by the smoothness of the initial distribution of the pump wave.<sup>14</sup> For a smooth initial Gaussian distribution decreasing fast toward the edges, the Fresnel number does not exceed 25–50, but the interaction of waves in the SHG process at the temperature distribution inhomogeneous over the beam cross section gives rise to small-scale inhomogeneities. Variations of the parameters  $G$  and  $N_{\xi,v}$  at solution of the system (7) showed that the values  $G = 4$  and  $N_{\xi,v} = 64$  and 128 are quite sufficient for realistic description of small-scale inhomogeneities of  $u_{1,2}(\xi, v)$  arising in the SHG process. Note that at these values of  $G$  and  $N_{\xi,v}$ , the fields of the pump and SH waves distort insignificantly in the process of propagation due to the limitedness of the Fourier spectrum. At  $\Delta\zeta = 0.05 - 0.1$  ( $N_z = 10 - 20$ ) the results of calculation of the conversion efficiency and the amplitude  $u(\zeta)_{1,2}$  for the case of no diffraction, homogeneous intensity distribution, and rectangular pulse of the pump wave agree well with the known analytical equations for this case.<sup>7</sup>

For solution of the heat conduction equation with the third-order boundary conditions we took the implicit alternating direction method<sup>15</sup> because of its simple program implementation. This method is characterized by the second order of accuracy with the error  $O[(\Delta\tau)^2, \Delta\xi^2, (\Delta v)^2]$  and is unconditionally stable. The time step for integration of the system (7) was chosen to be such that the field phase changes due to introduction of  $\zeta$  phase screens describing thermal blooming at every layer by a rather small value:  $\gamma\Delta T\Delta\zeta \leq 1$ . Then, taking into account the condition  $\Delta\zeta \leq 0.1$  and Eq. (6), we obtain

$$\Delta t \leq \frac{\rho C_p}{(2\pi/\lambda)\Delta\zeta\gamma L_z 2\delta_1 I_t(0)}. \quad (10)$$

From the inequality (10) it follows that  $\Delta t \leq 0.1 - 0.3$  s. For the considered initial data and types of crystals,  $\tilde{\tau}_T$  is 25–240 s. Therefore, if conditions (10) hold, the requirements of the small step in  $t$  are met from the viewpoint of the approximation error. The value of  $\alpha$  was taken equal to  $5 \cdot 10^{-2}$  W/(cm<sup>2</sup>·K), which corresponded to the conditions of contact heat removal.<sup>16</sup> The pump intensity was taken equal to the half surface damage threshold, thus providing for long and reliable operation of the frequency doubler.

### 3. Results on numerically simulated SHG

The calculations have been performed for the single pulse and repetitively pulsed modes on the assumption of the rectangular time shape of radiation pulses and rectangular intensity distribution in the cross section of the pump pulse, as well as for the Gaussian time shape of pulses and the Gaussian intensity distribution taking into account and neglecting the processes of temperature field establishment in a crystal. The following parameters of the pumping CO<sub>2</sub> laser were taken:  $\lambda = 9.55 \mu\text{m}$  [9P(20) line],  $E_p = 50 \text{ mJ}$ , the pulse repetition frequency up to 1 kHz.

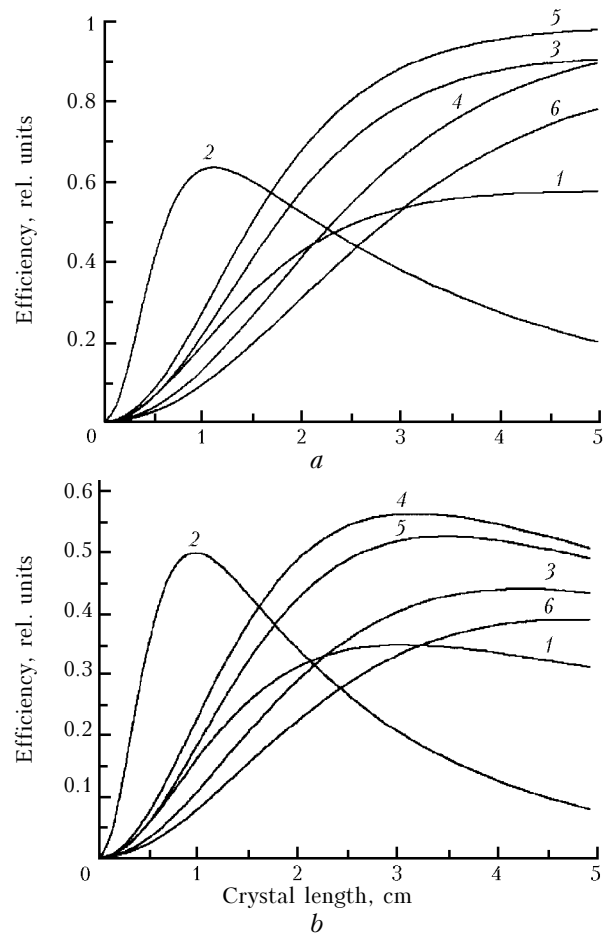
There exists a characteristic length of process development, at which the effect is accumulated up to a value affecting the conversion efficiency.<sup>7</sup> Leaving in the equations only the terms describing the corresponding effects and derivatives  $\partial A_{1,2} / \partial z$ , we can find the characteristic lengths of the processes by turns. The need in taking into account one or another effect in calculating the efficiency is determined by comparing the crystal length with the corresponding characteristic length of a process. Thus, for example, for the ZnGeP<sub>2</sub> crystal at the given parameters of the pump radiation, the nonlinear length is  $l_{nl} = (\sqrt{\sigma_1 \sigma_2 A^0})^{-1} = 0.8 \text{ cm}$ , the aperture length is  $l_w = 2w / \beta = 16 \text{ cm}$  ( $2w$  is the diameter of the input beam), and the diffraction length is  $l_d = 2\pi w_0^2 n / \lambda = 130 \text{ cm}$  ( $w_0$  is the radius of the Gaussian beam at the beam waist at the  $1/e$  intensity level).

Figure 2a depicts the SHG efficiency as a function of the length of the ZnGeP<sub>2</sub>, CdGeAs<sub>2</sub>, HgGa<sub>2</sub>S<sub>4</sub>, Tl<sub>3</sub>AsSe<sub>3</sub>, AgGaSe<sub>2</sub>, and GaSe crystals for the Gaussian time shape of the pulse and the Gaussian pump intensity distribution at the single pulse mode of conversion for pre-breakdown pump intensity. The pulse was divided into 16 layers in time. The experimentally determined values of the SHG efficiency in these crystals have been compared in Refs. 17 and 18.

Figure 2b depicts similar dependences but for the pump intensity of  $30 \text{ MW/cm}^2$  fixed for all the crystals. In SHG of TEA CO<sub>2</sub> lasers, ZnGeP<sub>2</sub> crystals have 1.8 times lower efficiency as compared with that of Tl<sub>3</sub>AsSe<sub>3</sub> and HgGa<sub>2</sub>S<sub>4</sub> crystals at the same pump intensity because of the higher level of optical loss. This loss restricts the maximum reasonable length of ZnGeP<sub>2</sub> crystals to  $\sim 2 \text{ cm}$ . As compared to AgGaSe<sub>2</sub> and GaSe crystals, the loss of the maximum achievable efficiency is 1.5 times.

The current state of the technology of growth of nonlinear crystals is such that in using crystals shorter than 1–2 cm, the ZnGeP<sub>2</sub> crystals occupied and occupy the second place in the SHG efficiency after the CdGeAs<sub>2</sub> crystals and excel all crystals in performance characteristics. With the today's level of technology development, the use of Tl<sub>3</sub>AsSe<sub>3</sub>, AgGaSe<sub>2</sub>, and HgGa<sub>2</sub>S<sub>4</sub> crystals more than 2 cm long and even GaSe

more than 5 cm long allows implementation of more efficient CO<sub>2</sub> laser SHG with the corresponding increase of the cost. The realistic level of the SHG efficiency is  $\geq 40\%$ .

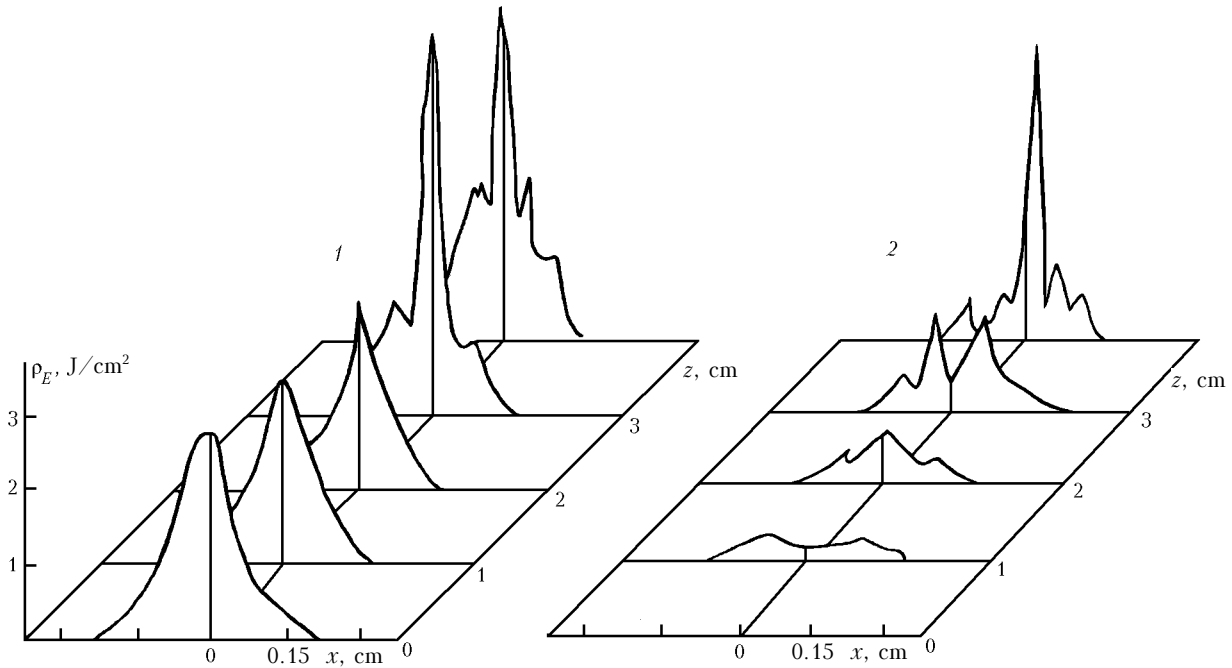


**Fig. 2.** Efficiency of CO<sub>2</sub> laser SHG vs. length of coated nonlinear element for ZnGeP<sub>2</sub> (1), CdGeAs<sub>2</sub> (2), AgGaSe<sub>2</sub> (3), HgGaS<sub>4</sub> (4), Tl<sub>3</sub>AsSe<sub>3</sub> (5), GaSe (6) crystals at pre-breakdown pump intensities (a) and pump intensity  $P = 3 \cdot 10^7 \text{ W/cm}^2$  (b).

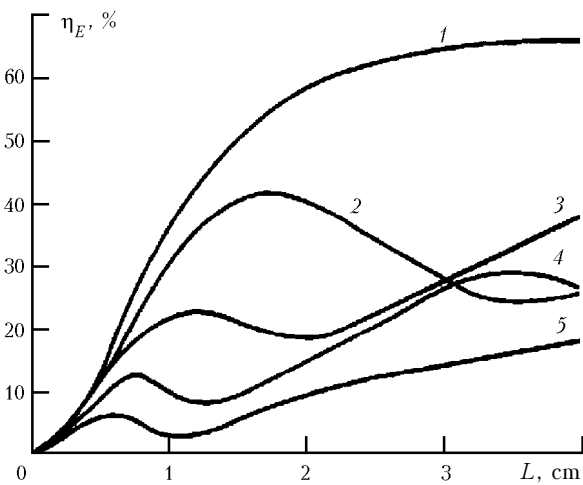
Some estimates for SHG of a repetitively pulsed CO<sub>2</sub> laser are depicted in Figs. 3–5. The SHG efficiency  $\eta_E$  in the cross section of the ZnGeP<sub>2</sub> crystal was calculated for the successive moments in time after the beginning of pump. Figure 3 depicts the calculated results for 0.5 s after the beginning of pump. It can be seen that the conversion efficiency varies with SHG evolution. The beams acquire ring structure varying in time. This is connected with the fact that the phase mismatch correlates with the temperature distribution over the beam cross section. Asymmetric transformation of the pump and SH beams is observed because of the effect of radiation walk off. The conversion efficiency becomes a complicated function of the crystal length, and its optimal length should be determined separately in every particular case. The necessary condition in this case is that the intensity at the exit surface of the crystal should not exceed the optical damage threshold.

Figure 4a demonstrates how the conversion efficiency changes with time. At a given pump pulse repetition frequency, there is an optimal (from the viewpoint of obtaining the maximum conversion efficiency for the SHG period) crystal length. The ZnGeP<sub>2</sub> crystal is characterized by the strong positive temperature dependence of the refractive indices at the pump and SH waves that leads to formation of a positive focusing lens. The intensities of the pump and SH waves on the crystal exit surface are shown in Fig. 4b.

The beams propagating in the crystal have a multifocal structure. As the crystal heats, the focus of the thermal lens for the pump and SH waves approaches the surface from the infinity and then moves further into the crystal. The focuses cross the rear edge of the crystal in turn: first that of the pump wave, then that of the SH wave, then the pump wave again, and so on. As the total intensity of the pump wave and the SH wave exceeds the surface damage threshold, the thermal self-focusing is an additional factor restricting the mean pump power.



**Fig. 3.** Evolution of thermal self-focusing in ZnGeP<sub>2</sub> crystal at SHG of CO<sub>2</sub> laser pulses with the repetition frequency of 1 kHz. Energy distribution cross sections for the pump wave (1) and SH (2) at propagation along the axis *z* 0.5 s after the beginning of pump.



**Fig. 4a.** Efficiency of conversion into the second harmonic vs. length of ZnGeP<sub>2</sub> crystal at pulse repetition frequency of 1 kHz at the successive moments in time 10<sup>-7</sup> (1), 0.1 (2), 0.25 (3), 0.5 (4), and 1 s (5).

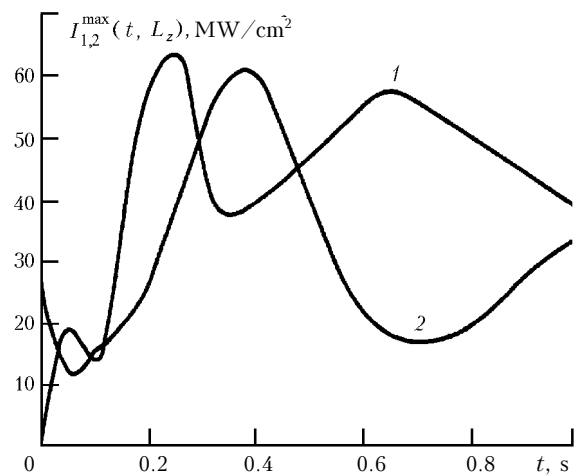


**Fig. 4b.** Time dependence of the maximum intensity of the pump wave (1) and SH (2) at the exit surface of ZnGeP<sub>2</sub> crystal 3.5 cm long at the pump pulse repetition frequency of 1 kHz.

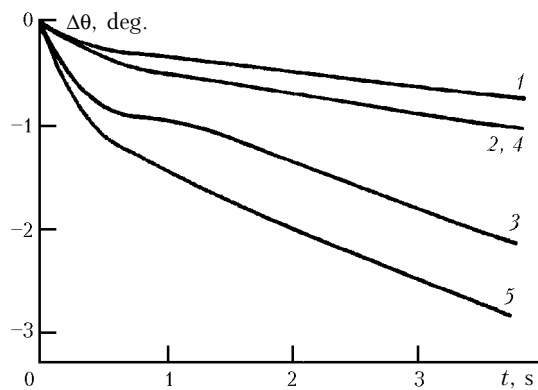


**Fig. 5.** Time dependence of the mismatch angle compensating for the effect of thermal self-focusing for SHG of 50 mJ pulses in  $\text{ZnGeP}_2$  crystals at the pulse repetition frequency of 400 Hz and the crystal length of 3.5 (1), 2.5 (2), and 1.5 cm (4), as well as 1 kHz and the crystal length of 2.5 (3) and 1 cm (5).

When the pulse repetition frequency decreases (this means that the mean pump power decreases too), the focus of the thermal lens is beyond the crystal and the radiation intensity on the rear surface does not exceed the surface damage threshold.

However, the development of thermal self-focusing leads to a decrease in the SHG efficiency and in the mean output power of SH. One of the ways to solve this problem may be compensation for the effect of thermal self-focusing by turning the crystal at some angle toward the direction of decreased mismatch as the crystal is heated. Figure 5 presents an example of the phase mismatch that provides for maximum SHG efficiency for the pump laser parameters specified above. Note that curves 2 and 4 in Fig. 5 that correspond to the crystal length of 2.5 and 1.5 cm almost coincide.

Sometimes, in the experiments, we used controlled heating of  $\text{ZnGeP}_2$  crystals to shift the phase-matching curves into the longwave spectral region. The reasonable limits of crystal heating did not exceed 160–200°C depending on the line of the pump  $\text{CO}_2$  laser.<sup>6</sup> At higher temperatures, the increase in the phonon absorption and the corresponding decrease in the SHG efficiency exceeded its growth due to a decrease in the phase-matching angle.

#### 4. Discussion

Having fixed some, for example 20%, decrease in the SHG efficiency and knowing the dependence of the SHG efficiency on the pulse repetition frequency, we can estimate the limiting mean pump power at partial compensation for the self-heating effect. In using the  $\text{ZnGeP}_2$  crystals of high optical quality and reasonable length of the nonlinear element (2–2.5 cm) the maximum pump pulse repetition frequency is 300 Hz. In the case considered, it corresponds to the mean pump power of 15 W and maximum SHG efficiency of 55%. In using crystals of moderate optical quality, these parameters are 10 W and 30% with the pulse repetition frequency of 200 Hz and the length of nonlinear elements of 1.5–2 cm.

Similar calculations were also performed for other nonlinear crystals. In the  $\text{AgGaSe}_2$  crystals of high optical quality, the 20% decrease in the SHG efficiency is observed at the maximum pump pulse repetition frequency of 400 Hz and the mean power of 20 W. The highest efficiency in this case is 50% with 5-cm long crystals. If crystals of a unique quality are used, the 20% decrease occurs at the pulse repetition frequency of 1 kHz and the mean pump power of 50 W, and the maximum efficiency achieves 53% with the crystals of the same length.

The  $\text{Tl}_3\text{AsSe}_3$  crystals are characterized by relatively low heat conductivity, and for the crystal sizes used in the calculations the time for establishment of the temperature distribution is 10 s. For these crystals in the case of a unique optical quality, the 20% decrease was observed for the maximum pump pulse repetition frequency of 500 Hz and mean power of 25 W. The maximum SHG efficiency was 55%, but for 9 cm long nonlinear elements. The  $\text{HgGa}_2\text{S}_4$  crystals were not considered in this case, because no correct data are available on their thermal and thermo-optical properties. When considering crystals of moderate optical quality, the high optical damage threshold and thermal parameters of the  $\text{ZnGeP}_2$  crystals turn out to be the decisive parameters.<sup>19</sup> In their potential, the  $\text{ZnGeP}_2$  crystals still yield to only the  $\text{CdGeAs}_2$  crystals cooled down to cryogenic temperatures, if the crystal length does not exceed ~2 cm. When using high-quality crystals, their thermal properties are no longer decisive, and 5–10-cm long samples of the  $\text{Tl}_3\text{AsSe}_3$ ,  $\text{AgGaSe}_2$ , and even GaSe crystals have maximum potential SHG efficiencies.

Note that when the walk off effect important for frequency conversion of small-aperture beams ( $w = 1\text{--}4$  mm) is taken into account,  $\text{AgGaSe}_2$  has an advantage over all other crystals. Small apertures are typical of mobile laser systems. Without antireflection coating, the SHG efficiency in the crystals considered is nearly halved, and this decrease is most significant for the  $\text{Tl}_3\text{AsSe}_3$  (2.4 times) and  $\text{CdGeAs}_2$  (2.2 times) crystals because of the high values of the refractive indices.

The SHG efficiency was also calculated for cw radiation and for short 1-ns duration pulses. In the former case, the conversion efficiency is the lowest in the  $\text{ZnGeP}_2$  crystals (only  $5 \cdot 10^{-4}\%$  at the pump intensity of  $2 \cdot 10^5 \text{ W/cm}^2$ ). However, if the walk off effect is taken into account, the situation changes drastically. In particular, for the GaSe crystals the maximum length is 2.7 mm for the beam diameter of 1 mm, and for the  $\text{Tl}_3\text{AsSe}_3$  crystals it is 5.5 mm. The real competitors to the  $\text{ZnGeP}_2$  crystals in this case are the  $\text{AgGaSe}_2$ ,  $\text{HgGa}_2\text{S}_4$ , and  $\text{CdGeAs}_2$  crystals due to high figure of merit. The advantage of one or another crystal in this case will be determined by the particular SHG scheme.

The extremely high conversion efficiencies up to 90% level and higher can be obtained in all nonlinear crystals of the mid-IR region pumped by radiation with the pulse duration  $\tau \approx 1$  ns. In this case, the length of the  $\text{CdGeAs}_2$  crystals should be within 2–3 mm, that of the  $\text{ZnGeP}_2$ ,  $\text{AgGaSe}_2$ ,  $\text{HgGa}_2\text{S}_4$ , and

$\text{Ti}_3\text{AsSe}_3$  crystals should not exceed 4–6 mm, and that of the  $\text{AgGaSe}_2$  and  $\text{GaSe}$  crystals should be 8–9 mm. In all the cases, the use of centimeter-long crystals makes no sense.

### Conclusion

The possibilities of creating second harmonic generators for TEA  $\text{CO}_2$  lasers with the mean output power up to tens of watts have been analyzed.

The system of connected equations for the amplitudes of the interacting waves has been solved along with the two-dimensional heat conduction equation, and this allowed us to take into account the thermal blooming effects at SHG.

The dependence of the efficiency on the crystal lengths for different crystals has been drawn with the allowance for optical quality of a crystal. The calculated results on the conversion efficiency in the case of no diffraction, homogeneous intensity distribution, and rectangular shape of the pump pulse agree well with the known analytical results for these conditions, thus confirming the correctness of the estimates obtained.

The angles of crystal turn that maximize the SHG efficiency and the optimal crystal lengths ensuring the highest SHG efficiency at the fixed pulse repetition frequency have been calculated. It has been found that the maximum SHG efficiency in  $\text{ZnGeP}_2$  is equal to 56% at the pulse repetition frequency of 300 Hz, and this value corresponds to the mean pump power of 15 W.

It has been shown that conversion of the repetitively pulsed radiation of the TEA  $\text{CO}_2$  laser without significant decrease in the efficiency due to thermal phase mismatch is possible in the  $\text{ZnGeP}_2$  crystal of good optical quality at the mean power up to 5 W and in the  $\text{AgGaSe}_2$  and  $\text{Ti}_3\text{AsSe}_3$  crystals up to 10 W. In the crystals of higher optical quality the mean power can be up to 10 and 20 W, respectively.

### Acknowledgments

The author is thankful to Yu.M. Andreev and A.V. Vernik for criticism and useful discussions.

### References

1. D.K. Killinger, N. Menyuk, and W.E. DeFeo, *Appl. Phys. Lett.* **36**, No. 6, 402–405 (1980).
2. N. Menyuk, D.K. Killinger, and W.E. DeFeo, *Appl. Opt.* **19**, No. 19, 3282–3286 (1980).
3. V.E. Zuev, M.V. Kabanov, Yu.M. Andreev, V.G. Voevodin, P.P. Geiko, A.I. Gribenyukov, and V.V. Zuev, *Izv. Akad. Nauk SSSR, Ser. Fiz.* **52**, No. 6, 1142–1149 (1988).
4. V.G. Dmitriev, G.G. Gurzadyan, and D.N. Nikogosyan, *Handbook of Nonlinear Optical Crystals* (Springer-Verlag, New York–Berlin–Heidelberg, 1999), 413 pp.
5. Yu.M. Andreev, V.V. Badikov, V.G. Voevodin, L.G. Geiko, P.P. Geiko, M.V. Ivashchenko, A.I. Karapuzikov, and I.V. Sherstov, *Kvant. Elektron.* **31**, No. 12, 1075–1078 (2001).
6. Yu.M. Andreev, L.G. Geiko, and P.P. Geiko, *Izv. Vyssh. Uchebn. Zaved., Fiz.*, No. 10, 85–89 (2002).
7. V.G. Dmitriev and L.V. Tarasov, *Applied Nonlinear Optics* (Radio i Svyaz, Moscow, 1982), 352 pp.
8. F. Zernike and J.E. Midwinter, *Applied Nonlinear Optics: Basics and Applications* (Wiley Interscience, New York, 1973).
9. S.A. Akhmanov and R.V. Khokhlov, *Problems of Nonlinear Optics (Electromagnetic Waves in Nonlinear Dispersive Media)* (VINITI, Moscow, 1965), 295 pp.
10. M. Okada and S. Ieiri, *IEEE J. Quant. Electron.* **7**, No. 9, 469–470 (1971).
11. V.G. Dmitriev, V.A. Konovalov, and E.A. Shalaev, *Kvant. Elektron.* **2**, No. 3, 496–502 (1975).
12. Yu.N. Karamzin, A.P. Sukhorukov, and V.A. Trofimov, *Mathematical Simulation in Nonlinear Optics* (Moscow State University Publishing House, Moscow, 1989), 154 pp.
13. S.S. Chesnokov, *Vestn. MGU, Fiz. Astronom.* **21**, No. 6, 27–31 (1980).
14. E.A. Ziklas and A.E. Siegman, *Appl. Opt.* **14**, 1874–1886 (1975).
15. D.A. Anderson, J.C. Tannehill, and R.H. Pletcher, *Computational Fluid Mechanics and Heat Transfer* (Hemisphere Publishing Corporation, New York, 1984).
16. G.N. Dul'nev, *Heat and Mass Exchange in Electronics* (Vysshaya Shkola, Moscow, 1984), 247 pp.
17. V.A. Gorobets, V.O. Petukhov, S.Ya. Tochitskii, and V.V. Churakov, *Opt. Zh.* **66**, No. 1, 62–67 (1999).
18. P.P. Geiko and Yu.M. Andreev, *Atmos. Oceanic Opt.* **13**, No. 12, 1060–1062 (2000).
19. Yu.M. Andreev, P.P. Geiko, A.V. Vernik, and L.G. Geiko, *Proc. SPIE* **4035**, 237–244 (2000).